UNIVERSITY OF PITESTI SCIENTIFIC BULLETIN
Faculty Of Mechanics And Technology AUTOMOTIVE series, year XXI, no. 25

DESIGN AND DYNAMIC ANALYSIS OF A POWERED WHEELCHAIR

Ionut GEONEA, Nicolae DUMITRU
University of Craiova, Romania,

Article history:
Received: 11.11.2015; Accepted: 12.02.2016.

Abstract: *This paper presents researches developed by authors to design a motorized robotic wheelchair for disabled people. These devices enable disabled people perform many activities of daily living thus improving their quality of life. Proposed solution uses for traction one DC motor with steps adjustable angular speed, and for steering one smaller motor. It is presented the kinematic scheme of the proposed transmission and kinematic analysis. It is developed a CAD model of the transmission, mounted on a wheelchair. They are made simulation in Adams, in order to verify the functionality of the proposed transmission. The obtained results validate proposed transmission model and enable success implementation of this transmission to a wheelchair experimental model.*

Keywords: wheelchair, design, kinematics, dynamics, differential transmission.

INTRODUCTION

There are many examples of assistive devices for people with manipulative and locomotive disabilities. These devices enable disabled people to perform many activities of daily living thus improving their quality of life. Disabled people are increasingly able to lead an independent life and play a more productive role in society. In the case of disabled children, such assistive devices have been shown to be critical to their cognitive, physical and social development [9].
Wheelchair is still the best transportation means for disabled people, since its invention in 1595 (called an invalids chair) for Phillip II of Spain by an unknown inventor. They have since evolved into complex multi-degree-of-freedom mechanical and electro-mechanical devices and robotic systems [2, 3, 5, 6, 10, 11 and 12].
Despite rapid scientific and technological progress, there has been very little innovation in wheelchair design over the last 200-300 years. The folding wheelchair came in 1933, and powered wheelchairs were developed in the early 1970s [7]. New materials such as plastics, fiber-reinforced composites and aluminum alloys have found their application into the design and manufacture of lighter, stronger and more reliable wheelchairs [9]. The wheelchair industry has also benefitted from the development of lighter, efficient, durable and reliable motors, better amplifiers and controllers and most important of all superior batteries.
Since the user is in physical contact with the chair for extended periods of time, the contact surfaces especially the seat, requires a certain degree of customization to ensure comfort. Commercially available standup wheelchairs afford better seating and reaching, relief from pressure sores, and better health. They also allow users to operate equipment designed to be operated by standing people and improve the quality of social interaction with non disabled standing people [18].
Conventional wheelchairs are difficult to maneuver in constrained spaces because they only have two degrees of freedom (forward/backward movement and steering). However, the Alexis Omnidirectional Wheelchair [10], TRANSROVR and the European TIDE Initiative OMNI Wheelchair [11] can move omni-directionally by adapting non-conventional wheels developed for use by robotic vehicles for this application [9].

A number of computer controlled wheelchairs have been developed in recent years, including the CALL Smart Chair, NavChair, TinMan and WALKY [5, 6, 10, 11]. Wheelchair systems with customized user interfaces, sensors and controllers, suitably integrated, can potentially make the operation of a wheelchair much simpler and make it more accessible to people with disabilities. Such chairs may use a wide variety of sensors ranging from ultrasonic range sensors [21], cameras, encoders, accelerometers, and gyroscopes and any desired input device (communication aids, conventional joysticks, switches, pressure pads, laser pointers, speech recognition systems and force reflecting joysticks [21]). Suitable control algorithms assist the user in avoiding obstacles, following features such as walls, planning collision-free paths and travelling safely in cluttered environments with minimal user input [16, 19].
While motorized wheelchairs with sophisticated controls are well-suited on prepared surfaces, most are unable to surmount common obstacles like steps and curbs. Special purpose aids [6], including stairway lifts [9], stair climbers [15, 20] and customized outdoor buggies have been developed for specific environments, but they are not versatile enough for multipurpose use. For example, a wheelchair that can go up and down any flight of stairs has remained an open research and development issue over the past couple of decades.
One approach to improve the mobility of a wheelchair by an order of magnitude involves the use of legs instead of wheels as locomotion elements. Advances in robotics have made it possible to build and control legged machines [17]. It is not difficult to imagine wheelchairs with legs climbing slopes, stepping over obstacles and walking on uneven terrain.
An alternative design for a wheelchair [19] for locomotion on uneven terrain tries to combines the advantages of legged locomotion (versatility, adaptability) with wheeled locomotion (reliability, superior stability). The hybrid system is more attractive than a walking chair because it relies on wheeled locomotion that is established to be reliable and safe. The legs are used as crutches and only when they are needed [9].
Many electric wheelchairs use some form of direct drive, involving belts, chains and/or gears. On a smooth level surface, relatively little torque is required to propel the wheelchair and occupant at constants speeds of up to 5 or 6 mph. If this were the only requirement, small motors of a few hundred watts capacity would serve. But wheelchairs must overcome obstacles, usually at low speed, climb substantial grades and accelerate at reasonable rate. All of these conditions demand high torque, most often at low speed. Thus, most powered wheelchairs are equipped with motors (and associated electronic controls), that are much larger than necessary for constant level propulsion and with poor efficiency most of the time since high torque is obtained only at low speed. To overcome this, a new infinitely variable automatic transmission, that automatically changes its speed ratio, in response to load torque being transmitted, is presented in [13].
Most majorities of electric power wheelchairs have two motors: one at each wheel. Like in the case of wheelchair where the occupant uses the hands to rotate the main wheels on each side, using knobs fixed to wheels, every maneuver is made by varying the relative angular motion of the wheels by each side. From the technical point of view this is called “differential driving”.
This research brings arguments for a mechanical transmission that achieves the differential movement, on which the traction and the steering components are controlled by separately motors with suitable synthesis to achieve the proper angular speed difference of wheels.

KINEMATICS OF WHEELCHAIR TRANSMISSION

Kinematic scheme of wheelchair transmission is presented in Fig.1. Shaft I is actuated by straight line displacement electric motor M_1, steering is performed by steering motor M_2 placed on shaft V.

Bevel gears, (10, 12) and (10', 12') are planetary gears and they are mounted on shafts (IV, III), respectively (IV', III'), with pins assembly. Bevel gears, (11, 13), and (11', 13') are rotate around their axis and they are satellites gears. Satellites gears are mounted on needle bearings to axes fixed on differential casing, and achieve a planetary motion. To calculate the transmission ratio, the principle of motion reversing is applied (Willis). To straight line displacement the traction wheels of the wheelchair rotate at the same angular velocity. The motion is transmitted from worm gears 6-5 to the shaft II and by means of final transmission gears 4-2 to wheels.

For steering, the motion is transmitted from motor M_2 to shaft V, trough bevel gears (8, 9), (10, 11), (11, 12) to semi-axis III, respectively to motor wheel Rd. For left wheel Rs the transmission flow go through bevel gears (8, 9'), (10', 11'), (11', 12') to semi-axis III'. Those two wheels Rd and Rs will rotate with the same angular speed and opposite rotation sense. Casing S, S' and spur gear (2, 2') do not rotate (the motor M_1 is turned off).

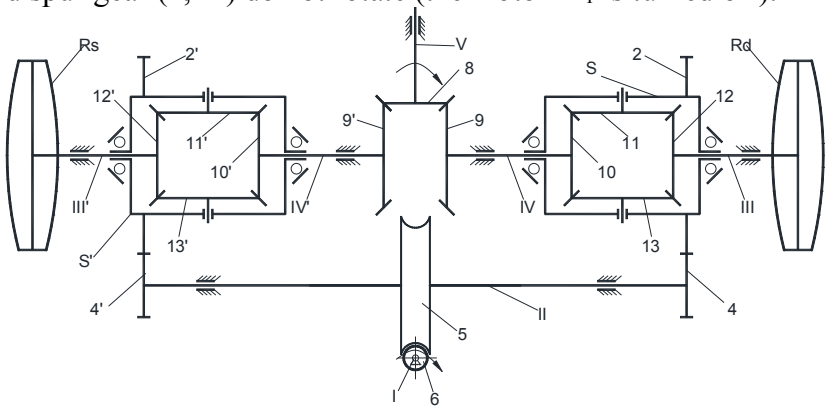

Figure 1. Kinematics scheme of wheelchair transmission

Transmission ratios

The motion transmission chain for straight line displacement of the wheelchair is expressed by relation (1), and for steering the motion transmission chain is expressed by relation (2).

$$\begin{aligned} &M_1 - I - i_{65}^{w} - II - i_{42}^{c} - III - Rd \\ &M_1 - I - i_{65}^{w} - II - i_{4'2'}^{c} - III - Rs \end{aligned} \tag{1}$$

Where: M_1- traction motor; i_{65}^{w}-worm gear ratio; i_{42}^{c}-final transmission ratio; Rd and Rs, right and left wheel, I, II and III – shafts.

$$\begin{aligned} &M_2 - V - i_{89}^{k} - IV - i_{10\,11}^{k} - i_{11\,12}^{k} - III - Rd \\ &M_2 - V - i_{89'}^{k} - IV' - i_{10'\,11'}^{k} - i_{11'\,12'}^{k} - III' - Rs \end{aligned} \tag{2}$$

where: M_2- steering motor; i_{89}^{k} $i_{89'}^{k}$-bevel gear ratio; $i_{10\,11}^{k}$-bevel gears 10, 11 ratio; $i_{11\,12}^{k}$-bevel gears 11, 12 ratio; Rd and Rs, right and left wheel, III, IV and V – shafts.

For wheelchair straight line displacement when booth drive wheels encounter the same resistance to ground, is valid relation (1). For steering, the governing equations of the wheels angular velocity are deducted in the following. Used notations are described below:

ω_{10}, ω_{12}-absolute angular velocity of bevel planetary gears 10 and 11, considered in relation to differential casing;

$\omega_{10}^{S} = \omega_{10} - \omega_{S}$-relative angular velocity of gear 10, towards differential casing S;

$\omega_{12}^{S} = \omega_{12} - \omega_{S}$-relative angular velocity of gear 12, towards differential casing S;

ω_{11}, ω_{13}- is relative angular velocity of satellite gears 11 and 13, towards differential casing S.

ω_S - is absolute angular velocity of differential housing upon wheelchair frame.

R_W -is the rolling circle radius for planetary gears 10 and 12.

r_W - rolling circle radius for satellites gears 11 and 13.

According to the principle of gearing, the tangential velocities are equal in the gearing point:

$$-(\omega_{10}-\omega_s)R_W=\omega_{11}r_W=(\omega_{12}-\omega_S)R_W=\omega_{13}r_W \tag{3}$$

We obtain:

$$\omega_s=\frac{\omega_{10}+\omega_{12}}{2} \tag{4}$$

Namely, the angular velocity of the central gear (planetary) is twice the angular velocity of the differential box. If the steering motor is turned off, then $\omega_{10}=0$, from Eq. (4) we obtain:

$$\omega_{12}=2\omega_s=2\omega_2 \tag{5}$$

In the same way: $\omega_{10}^{'}=0$, we obtain

$$\omega_{12'}=2\omega_{S'}=2\omega_{2'} \tag{6}$$

Taking into account the gears ratio, we write the equation:

$$\omega_s=\frac{\omega_{M_1}}{i_{65}^{w}\cdot i_{42}^{c}}\left[rad/s\right] \tag{7}$$

Where:

ω_{M_1} -is traction motor angular velocity; i_{65}^{w}-worm gear ratio; i_{42}^{c} -spur gears 4-2 transmission ratio.

In case of curve displacement of wheelchair, we have the equation:

$$\omega_{10}=\frac{n_{M_2}}{i_{89}^{k}};\ \omega_{10}{}'=\frac{n_{M_2}}{i_{89'}^{k}} \tag{8}$$

Assume that the right wheel Rd is outside the curve, in this case the pairs of satellite gears (11, 13) respectively (11', 13') rotate. Is distinguished: the absolute motion of planetary gears, transportation movement of differential box and relative movement of satellites gears towards differential box S or S'. In this context, the distribution of velocities in absolute motion of a planetary gear, is:

$$\omega_{10}\cdot R_W=\omega_S\cdot R_W+\omega_{11}\cdot r_W \tag{9}$$

If we take into account the relationship (4), we obtain the angular velocities for satellite gear (11) and planetary gears (10) and (12):

$$\omega_{11}=(\omega_{10}-\omega_s)\frac{R_W}{r_W},\ \omega_{10}=\omega_s+\omega_{11}\frac{r_W}{R_W},\ \omega_{12}=\omega_s-\omega_{11}\frac{r_W}{R_W} \tag{10}$$

DESIGN OF WHEELCHAIR TRANSMISSION CAD MODEL

Based on the kinematic scheme of the transmission (Figure 1) we achieved the design calculations of gears. Input data, respectively powers and angular speeds on shafts are known,

kinematic and dynamics parameters being establish. We calculate geometric elements of gears, upon we design the 3D models of gears, with GearTrax and Solid Works software. Also we performed transmission shafts and bearings calculation. These data allowed us to realize the 3D model of designed transmission on wheelchair, which are presented in Figure 2 and Figure 3. Differential transmissions have been fitted on the wheelchair structure, the assembly view being presented in Figure 3. The weight of the entire assembly is 45 kg.

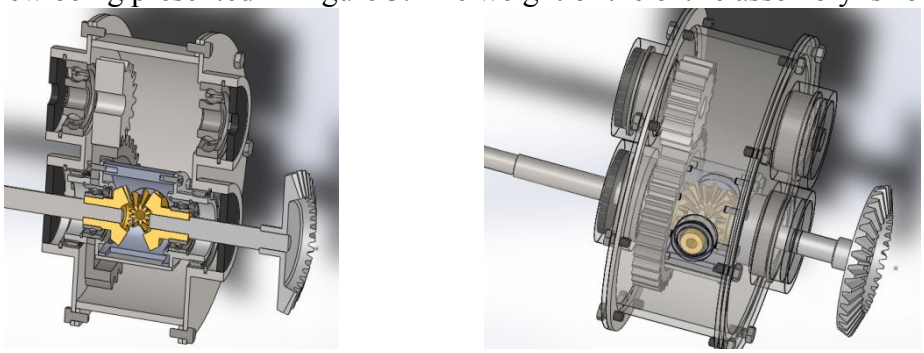

Figure 2. CAD model of differential transmission

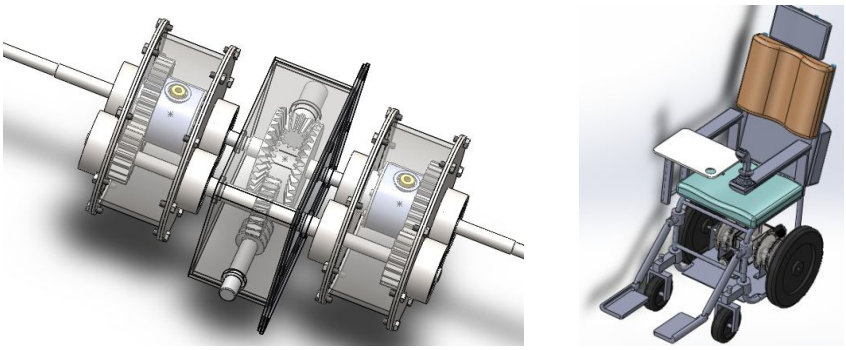

Figure 3. Wheelchair transmission assembly

MULTI-BODY DYNAMICS MODEL OF WHEELCHAIR

The virtual prototype of the wheelchair, as modeled in Fig. 3, is transferred into Adams multi-body model, using the transfer interface embedded in Solid Works. Trough a suitable modeling we perform the dynamic simulation of wheelchair assembly. Steps taken to completely define the dynamic model consist in: specify of kinematic elements mass properties, define of kinematics joints, specify of friction models (friction to joints, and wheels-ground contact), specify of human load by 70 kg and define of gear type connections (by defining the contact between gears solids).

The contact forces in the gear set are described by a contact mechanics model which is determined by parameters such as stiffness, force exponent, damping and friction coefficients, penetration depth. Msc.Adams has the capability of rigid-elastic model computation, which is suitable for the multi-body model of the gearbox. The rigid-elastic model is a compromise between the rigid body and elastic body, in which the shafts and gears body are taken as rigid, but the contact surfaces of the meshing gears are deformable bodies.

Contact parameters

Considering the computing efficiency and accuracy, is adopted the impact method to define gears contact. Necessary parameters for this method are shown in Fig. 4. The contact force computed by this method is composed of two components, the elastic force caused by the deforming components and the damping force caused by the relative deforming velocity.

The contact between ground and wheels, is specified according to the literature: Ψ_a - 0,5..0,6 for old asphalt road, old concrete. It should be noted that the front wheels are self-directed, being modeled by rotation joints with friction.

Establish of the parameters for a gearing pair contact model

The contact force model is shown in Fig.4. The contact force in Adams [8] can be expressed as:

$$F = \begin{cases} K\left(x_0 - x\right)^e + CS\dot{x} & x < x_0 \\ 0 & x \geq x_0 \end{cases} \tag{11}$$

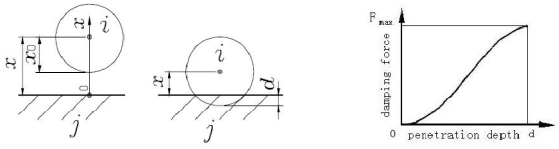

Figure 4. Contact force model in Adams [8]

In Eq.(11), x_0-x is the deformation in the process of contact-collision. Eq.(11) shows that the contact does not occur while $x \geq x_0$ and the contact force is zero. Contact occurs while $x < x_0$ and the contact force is related to the parameters such as stiffness K, the deformation x_0-x, contact force exponent *e*, damping coefficient *C* and the penetration depth *d* which is the maximum value of x0-x. *S* is a step function defined as (12):

$$S = \begin{cases} 0 & x < x_0 \\ \left(3 - 2\Delta d\right)\Delta d^2 & x_0 - d < x < x_0 \quad \cup \Delta d = x_0 - x \\ 1 & x \leq x_0 - d \end{cases} \tag{12}$$

In Eq. (12), $\Delta d = x_0$-x, is the deformation of the body. Eq. (11) also shows that the contact force defined in Adams is composed of two parts. An elastic component $K(x_0\text{-}x)e$, acts like a nonlinear spring. The other is the damping force CS(dx/dt), which is a function of the contact-collision velocity. By the definition of the step function in Eq.(12) we know that the damping force is defined as a cubic function of penetration depth. To avoid the function discontinuity caused by the dramatic variation of the damping force while contact-collision occurs, as shown in Fig.4, the damping force is set to zero when the penetration depth of the two contacted bodies is zero, and approaches a maximum value F_{max} when the specified penetration depth d is reached.

a)Stiffness K: according to the Hertzian elastic contact theory [8], the stiffness of two contacted bodies could be described by a pair of ideal contacted cylindrical bodies, from the equivalent radius of engaged helical gear pair. Consequently, the stiffness could be expressed as:

$$\begin{aligned} K &= \frac{4}{3} R^{\frac{1}{2}} E^* = \frac{4}{3}\left[\frac{id_1 \cos\alpha_t \tan\alpha_t'}{2\left(1+i\right)\cos\beta}\right]^{\frac{1}{2}} E^* \\ \frac{1}{E^*} &= \frac{1-\upsilon_1^2}{E_1} + \frac{1-\upsilon_2^2}{E_2} \\ \beta_b &= a\tan\left(\tan\beta\cos\alpha_t\right) \end{aligned} \tag{13}$$

Where: d_1-diameter of standard pitch circle; *i*-gear ratio; E_1, E_2- Young's modulus of two contacting bodies; E* -equivalent Young's modulus; α_t', α_t - transverse pressure angle at engaged, standard pitch circle; υ_1, υ_2-Poisson ration of the pinion and gear; β, β_b-helical angle at the pitch, base circle.

The materials for the pinions and gears of the transmission are alloy steel and the values for the Poisson ratio and the Young's modulus are: $\upsilon = 0.3$ and $E = 2.1 \cdot 10^5 N/mm^2$. Trough calculations, the stiffness values for the gear pairs in the drive line are inserted in the model, see Figure 4.

b) Force exponent: Considering numerical convergence and computation speed, a force exponent *e*=1.5 is determined [8].

c) Damping coefficient C, generally takes values 0.1%~1% of the stiffness K. For this simulation the damping coefficient is set to C=1000Ns/mm.

d) Penetration depth: The relationship between damping force and penetration depth is shown in Fig.4. In common cases, a reasonable value for penetration depth is 0.01 mm. We used d=0.1, considering the numerical convergence in Adams.

e) Dynamic and static friction coefficient and viscous velocity. The materials for the engaged gears are alloy steel and the meshing pairs are lubricated. Typical values found in mechanical design handbooks are: static friction coefficient $\mu_s = 0.1$; static transition velocity $v_s = 1mm/s$, dynamic friction coefficient $\mu_d = 0.08$ and friction transition velocity $v_d = 10mm/s$.

In Figure 5 are presented the specified parameters for one contact and friction model.

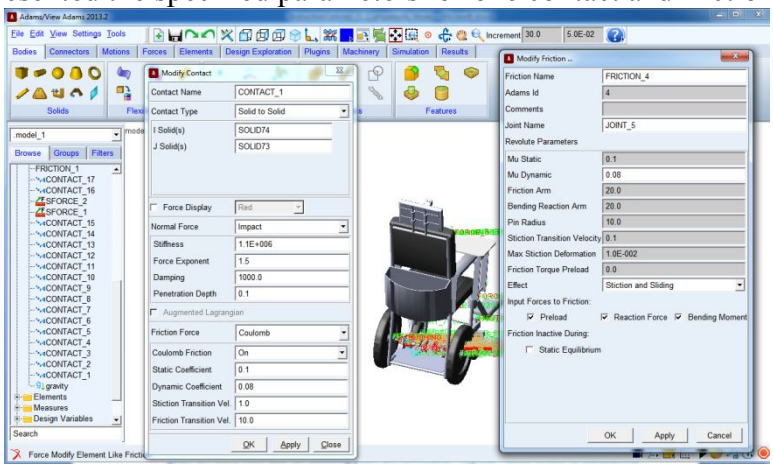

Figure 5. Wheelchair contact and friction parameters

It is achieved robotic system workspace analysis in Adams, in two assumptions: a combined trajectory composed of a straight line motion with steering and only steering motion active for displacement in a circle. In the first case there are active booth motions, straight line and steering. Functions used in Adams to define straight line motion and steering motion are given by Eq. 14.

$$\begin{aligned} &IF(\,time-2:\ 36.9\,,\ 0, IF(time-4:0\,,\ 36.9, 36.9)\,) \text{ –for traction motion (shaft I)} \\ &IF(\,time-2:\ 0\,,0\ ,\ 3.6\,) \text{ – for steering motion (shaft V)} \end{aligned} \tag{14}$$

In the second case of wheelchair simulation, is active only the steering motion, with value $\omega_2 = 8 \text{ rad/sec}$ (applied to shaft V). The simulation was achieved using WSTIFF solver with SI2 integration. The wheelchair motions trajectory obtained in both cases are presented in Figure 6.

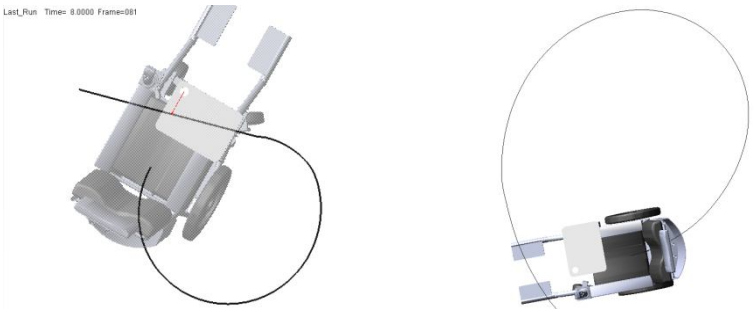

Figure 6. Wheelchair trajectory: combined motion and steering motion.

In case of combined traction and steering motion simulation, is obtained the right and left wheel angular velocity (respectively, planetary gear 12 and 12'), presented in Figure 7.

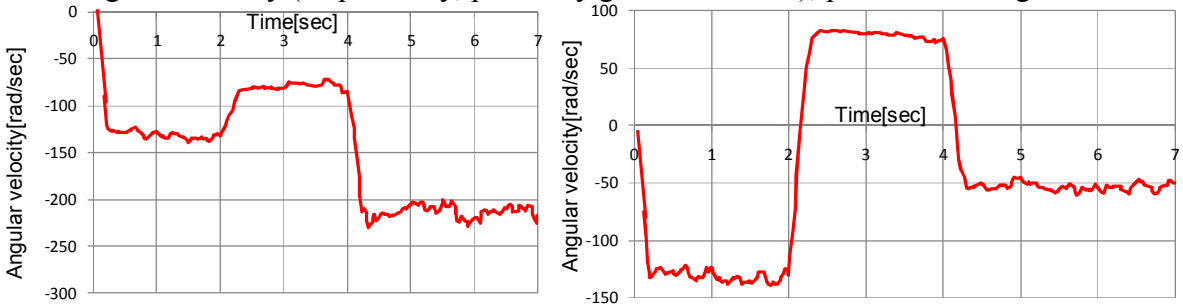

Figure 7. Right and left wheel angular velocity, in case of combined motion

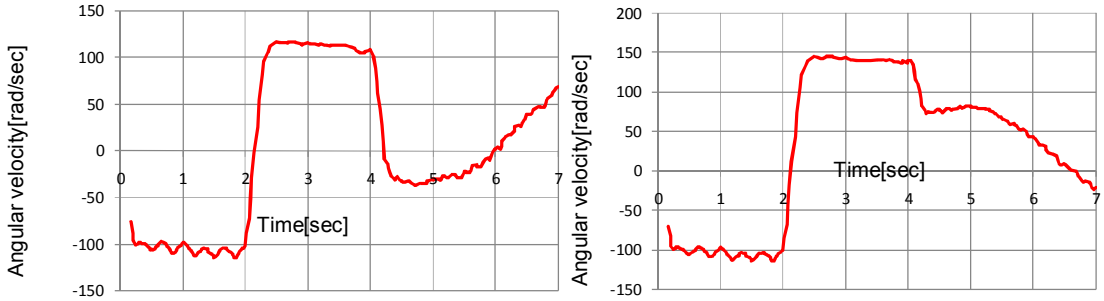

Figure 8. Satellite gear 11 and 11' angular velocity, in case of combined motion

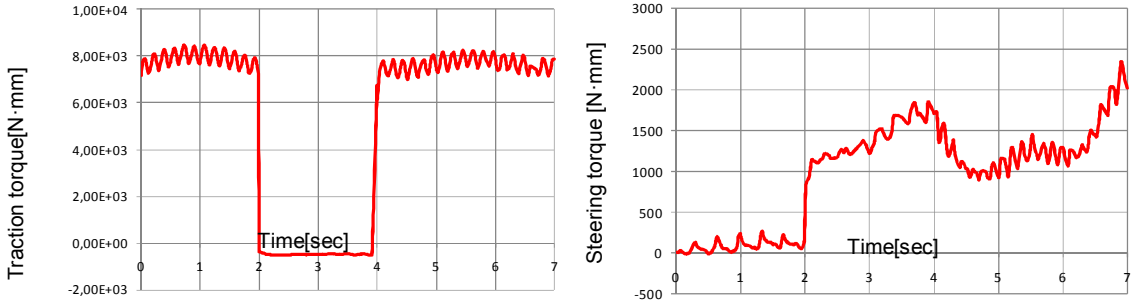

Figure 9. Traction and steering torque variation, in case of combined motion

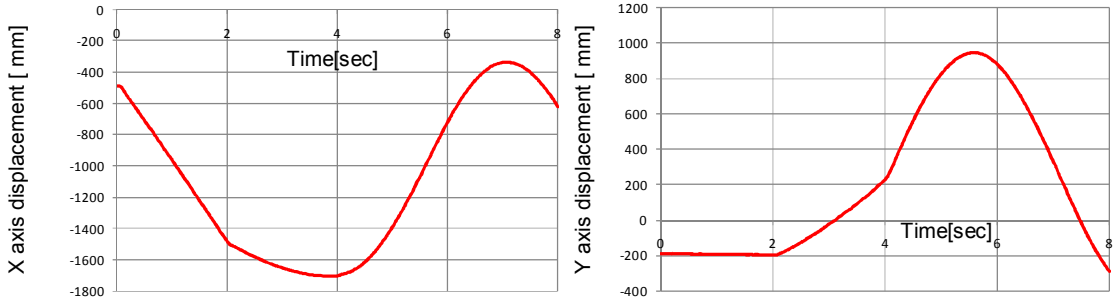

Figure 10. Wheelchair translational displacement upon X and Y axis

In case of combined motion trajectory, the wheelchair displacement upon X and Y axis are shown in Fig. 10, and resulting displacement and linear velocity magnitude are shown in Fig.11.

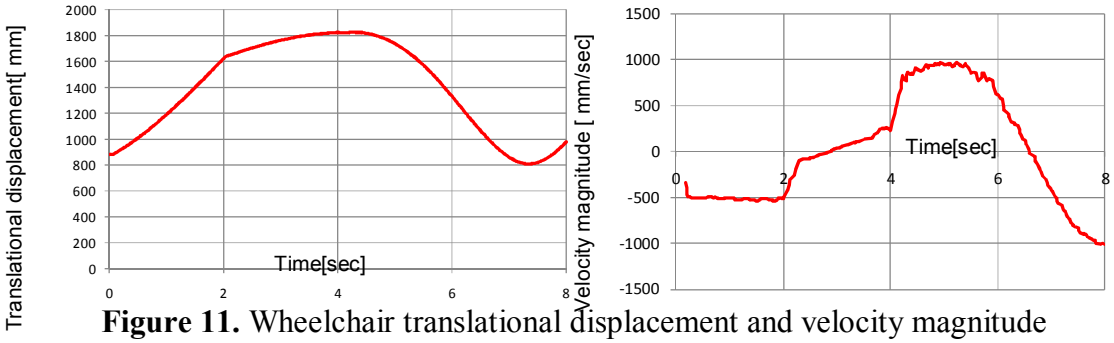

Figure 11. Wheelchair translational displacement and velocity magnitude

In case of steering motion simulation, is obtained the right and left wheel angular velocity (respectively, planetary gear 12 and 12'), presented in Figure 12.

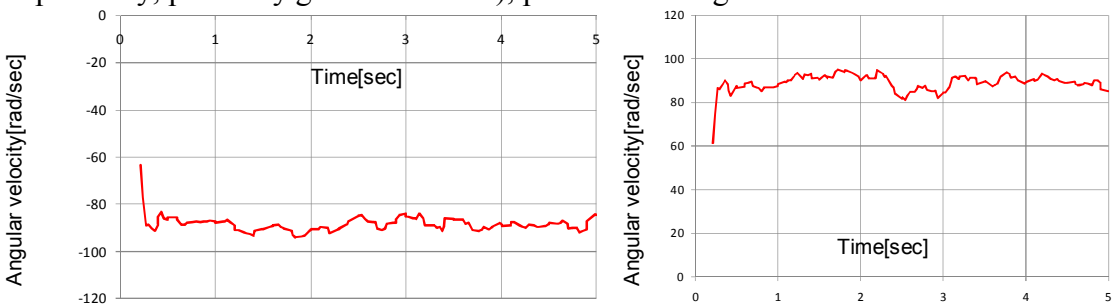

Figure12. Right and left wheel angular velocity, in case of steering motion

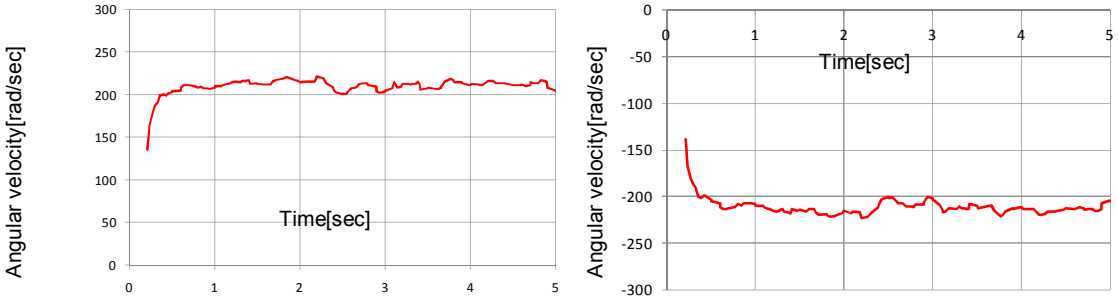

Figure 13. Satellite gear 11 and 11' angular velocity, in case of steering motion

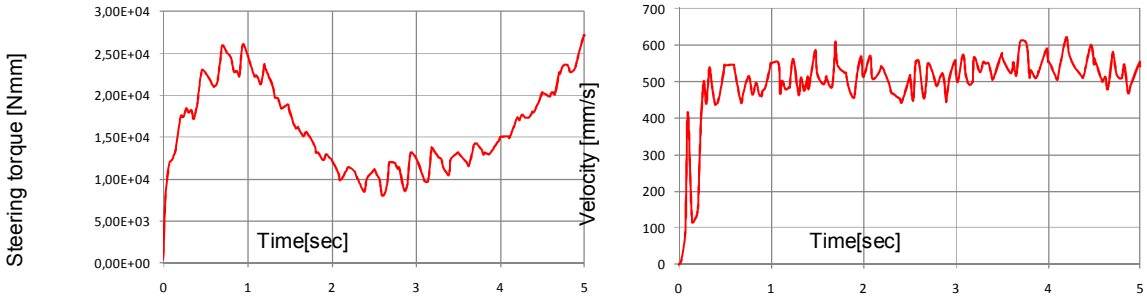

Figure 14. Steering torque variation and translational velocity magnitude

The wheelchair steering torque and translational velocity magnitude in case of steering motion trajectory are shown in Figure 14.

CONCLUSIONS

In this paper is achieved the design solution of a robotic wheelchair. For straight line motion and steering the wheelchair uses a transmission with differential gearboxes. Based on the

CAD modeling, it is developed a dynamic simulation in Adams, in order to validate the wheelchair prototype. The simulation is achieved in the case of a combined straight line and steering motion and it is presented the wheelchair motion trajectory, gears angular velocity, wheelchair translational displacement and velocity as well as traction and steering torque. Is observed that the traction torque of the wheelchair, caring a 70 kg human, is 8 Nm and the steering torque is by 30 Nm. Dynamic simulation performed in Adams demonstrates the efficiency of the proposed wheelchair transmission.

Acknowledgments: This work was supported by the strategic grant POSDRU/159/1.5/S/133255, Project ID 133255 (2014), co-financed by the European Social Fund within the Sectorial Operational Program Human Resources Development 2007-2013.

REFERENCES

[1] Dumitru, N.; Malciu, R., Geonea, I., *Differential Transmission for Robotizing a Powered Wheelchair*, Proceedings of the OPTIROB, 28-30 May 2010, pp. 47-51, ISBN 978-981-08-5840-7.
[2] Ekachai Ch., *A Prototype of a Stair-Climbing System for a Wheelchair*, The Second TSME International Conference on Mechanical Engineering, Thailand, 19-21 October, 2011.
[3] Gonzalez-Rodriguez Antonio, *Mechanical Synthesis for Easy and Fast Operation in Climbing and Walking Robots*, Climbing and Walking Robots, 2010, Available from: www.intechopen.com.
[4] Gurpude Rahul, Design, *Synthesis & Simulation Of Four Bar Mechanism For Guiding Wheel For Climbing*, International Journal of Engineering Research and Applications, 2012.
[5] Hassan Abdulkadir, *Design and Fabrication of a Motorized Prototype Tricycle for the Disable Persons*, IOSR Journal of Engineering May. 2012, Vol. 2(5), pp.1071-1074.
[6] Hidetoshi Ikeda, *Step Climbing and Descending for a Manual Wheelchair with a Network Care Robot*, The Second International Conference on Intelligent Systems and Applications, 2013.
[7] Kumar Vijay, *Assistive Devices For People With Motor Disabilities*, Wiley Encyclopedia of Electrical and Electronics Engineering Assistive Devices For People With Motor Disabilities, 1997.
[8] Kong D., J. M. Meagher, C. Xu, X. Wu, and Y. Wu, *Nonlinear Contact Analysis of Gear Teeth for Malfunction Diagnostics*, Conference and Exposition on Structural Dynamics, 2008.
[9] Modak G. S., *Review Article: Evolution of a Stair-Climbing Power Wheelchair*, IOSR Journal of Mechanical and Civil Engineering (IOSR-JMCE) ISSN(e): 2278-1684, ISSN(p), pp. 36-41.
[10] Pires G., Autonomous Wheelchair for Disabled People, Proc. IEEE Int. Symposium on Industrial Electronics (ISIE97), Guimarães, 797-801, 1997.
[11] Rajasekar R., *Design and fabrication of staircase climbing wheelchair*, Int. J. Mech. Eng. & Rob. Res., 2013.
[12] Razak S., *Design And Implementation Electrical Wheel Chair For Disable Able To Stairs Climbing By Using Hydraulic Jack*, IOSR Journal, Volume 7, Issue 3 (Sep.-Oct. 2013), pp.82-92.
[13] Reswick JB., *Automatic transmission for electric wheelchairs*, J. Rehabil. Res. Dev., 1985.
[14] Salmin Humaira, *Design and Implementation of an Electric Wheel-Chair to Economize it with Respect to Bangladesh*, International Journal Of Multidisciplinary Sciences And Engineering, 2014.
[15] Shanu Sharma, *User Centric Designed Mechanism For stairs-climbing Wheelchair*, 15th National Conference on Machines and Mechanisms NaCoMM, 2011.
[16] Sheng Lin Jzau, *Wireless brain computer interface for electric wheelchairs with EEG and eye-blinking signals*, International Journal of Innovative Computing, Information and Control, 2012.
[17] Sugahara Yusuke, *A Novel Stair-Climbing Wheelchair with Variable Configuration Four-Bar Linkage* - Mechanism Design and Kinematics-ROMANSY 18, Volume 524, pp. 167-174, 2010.
[18] Tianxiang Mo, *New Mechanism Used in Standing Wheelchair*, Science Thesis in Mechanical Engineering, Karlskrona, Sweden, 2014.
[19] Walter de Britto Vidal Filho, *Mechatronic design of a chair for disabled with locomotion by legs*, ABCM Symposium Series in Mechatronics - Vol. 5, 2012.
[20] Wellman, P., V. Krovi, V. Kumar and W. Harwin, *Design of a Wheelchair with Legs for People with Motor Disabilities*, IEEE Transactions on Rehabilitative Eng. Vol. 3, pp.343-353, 1995.
[21] Wolm P., *Dynamic stability control of front wheel drive wheelchairs using solid state accelerometers and gyroscopes*, PhD Thesis, University of Canterbury, 2009.
[22] MSC Inc., *MSC Adams 2013 reference manual*.